Available online at www.sciencedirect.com
ScienceDirect
Trans. Nonferrous Met. Soc. China 20(2010) 2209−2214
Transactions of Nonferrous Metals Society of China
www.tnmsc.cn

Effects of precipitates on fatigue crack growth rate of AA 7055 aluminum alloy

CHEN Jun-zhou(陈军洲)[1], ZHEN Liang(甄 良)[2], YANG Shou-jie(杨守杰)[1], DAI Sheng-long(戴圣龙)[1]

1. Beijing Institute of Aeronautical Materials, Beijing 100095, China;
2. School of Materials Science and Engineering, Harbin Institute of Technology, Harbin 150001, China

Received 13 July 2009; accepted 4 January 2010

Abstract: The effects of precipitates on the fatigue crack growth rate of AA 7055 Al alloy subjected to different ageing treatments were investigated using transmission electron microscope and fatigue crack growth testing. The results show that the T77 treated samples exhibit the lowest crack growth rate, while the crack growth rate of over-aged samples is the highest. In terms of the model based on the reversibility of dislocation motion within the plastic zone close to the crack tip, the improved crack growth resistance is attributed to many precipitates that are coherent with Al matrix in the under-aged and T77 treated samples. When the precipitate is coherent with the Al matrix, the larger the precipitate is, the slower the fatigue crack grows. The effects of grain boundary precipitates and precipitate free zone on the fatigue crack growth resistance are less significant than those of precipitates within grains of the alloy.

Key words: 7055 aluminum alloy; ageing; fatigue crack growth rate; precipitate

1 Introduction

Based on the principles of aircraft design, the higher fatigue crack growth resistance of advanced aluminum alloys is required and paid much attention considering their higher damage tolerance and higher life-cycle[1]. It is well accepted that microstructures, such as grain size[2], orientation[3−4], secondary phases[5−6] and precipitates[7−8], can affect the fatigue crack growth behavior of aluminum alloys. For the age-hardenable aluminum alloys, the effect of precipitates is most important. As one of advanced age-hardenable aluminum alloys, 7055 aluminum alloy has been widely applied as the upper-wing structural material of commercial aircrafts due to its high strength, high fracture toughness and improved corrosion resistance[9−12]. According to Refs.[13−16], the crack growth rates of some aluminum alloys corresponding to a given $\Delta K = 10\text{MPa}\cdot\text{m}^{-1/2}$, stress ratio $R = 0.1$, are as follows: -1.0×10^{-4} mm/cycle for 7475-T7351 alloy[13]; -1.5×10^{-4} mm/cycle for 7050-T7451 alloy[14]; -2.0×10^{-4} mm/cycle for 7055-T7751 alloy[15]; -2.0×10^{-4} mm/cycle for 2024-T351 alloy [16].

It can be seen that these improved properties are achieved without much loss in the fatigue crack growth resistance for 7055 aluminum alloy. The correlations between the microstructure and strength or fracture toughness have been studied for this alloy. SRIVATSAN and SRIRAM[12] first reported the detailed microstructures and their influences on the tensile deformation and fracture behavior of 7055 Al alloy. Based on microstructure information, DIXIT et al[17] utilized existing models to predict strength and fracture toughness for 7055 Al alloy. The predicted values are close to the experimentally reported ones. However, few work was published for the correlations between precipitates and fatigue crack growth in this advanced Al alloy. In our previous work[18], although the fatigue crack growth behavior of 7055 Al alloy with under-ageing and peak ageing was introduced, it is still unknown why 7055-T7751 aluminum alloy shows such a good fatigue crack growth resistance.

In this study, the fatigue crack growth rates of 7055 aluminum alloy under four typical ageing conditions were measured. The microstructures of the alloys under the corresponding conditions were characterized with transmission electron microscopy (TEM), high

Foundation item: Project(2005CB623700) supported by the National Basic Research Program of China
Corresponding author: CHEN Jun-zhou; Tel: +86-10-62496396; E-mail: junzhouchen@126.com
DOI: 10.1016/S1003-6326(10)60630-9

resolution transmission electron microscopy (HRTEM) and selected area electron diffraction (SAED) technique to further understand the effects of precipitates on the fatigue crack growth in this alloy.

2 Experimental

The 7055 Al alloy used in this work was provided by ALCOA (Aluminum Company of America) as 19 mm thick rolled plate in T77 temper. Its chemical composition is Al-7.8Zn-1.9Mg-2.4Cu-0.12Zr-0.06Fe-0.06Si-0.005Cr-0.008Mn (mass fraction, %). T77 is proprietary temper alloy designated by ALCOA, which involves solution heat treatment, water quench and a permanent stretch prior to three-step artificial ageing. The as-received rolled plates were solid solution treated at 477 °C for 1 h, followed by water quenching. In order to study the effects of microstructure on the fatigue crack growth rate, the plates were one-step aged after quenching at 120 °C for 1 and 24 h and at 160 °C for 24 h, respectively. These three conditions were corresponding to under-ageing (UA), peak-ageing (PA) and over-ageing (OA), respectively. The mechanical properties of the alloy under different conditions are shown in Table 1.

Table 1 Mechanical properties of alloy under different conditions

Condition	$\sigma_{0.2}$/MPa	σ_b/MPa	δ/%
Over-ageing	513	552	17
Peak-ageing	525	584	21
Under-ageing	465	568	26
T77	576	592	17

Fatigue crack growth tests were undertaken in agreement with ASTM E647 standard using middle-tension (M(T)) 6 mm thick specimens. The specimens were machined from the longitudinal transverse direction of the as-received and heat treated plates at the same position. Fig.1 shows the dimensions of the samples used in the test. The samples were mechanically polished. Three samples were prepared for each ageing condition. All experiments were conducted at room temperature in air on a closed-loop servohydraulic machine at a frequency of 10 Hz and a stress ratio (R) of 0.06. The constant amplitude tests were performed in load control mode. The fatigue crack growth rate (da/dN) data were generated using the K-increasing procedure for da/dN > 1×10^{-5} mm/cycle. The crack lengths were measured by a traveling optical microscope.

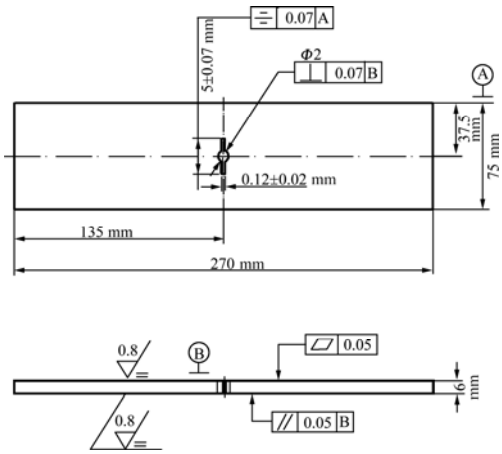

Fig.1 Dimensions of M(T) specimen

Thin foils for TEM observation were prepared from discs with diameter of 3 mm punched from 0.5 mm thick slices cut from fatigue crack growth samples after testing, mechanically ground and thinned by twin-jet electropolishing in a 30% Nital solution at −20 °C and a potential difference of 15 V. TEM and HRTEM examinations were performed by using a JEM 2010 microscope operating at 200 kV.

3 Results

Fig.2 shows the fatigue crack growth rate for the alloys in different ageing conditions. The obtained values of da/dN are plotted against ΔK. The linear portions of the curve, i.e. the Paris region, are found to follow the following equation:

$$\frac{\mathrm{d}a}{\mathrm{d}N}=C(\Delta K)^n \tag{1}$$

where C and n are the Paris constants, respectively, and ΔK is the stress intensity factor range. In the present work, the fatigue crack growth rate is studied in this region. Table 2 shows the da/dN values at given ΔK

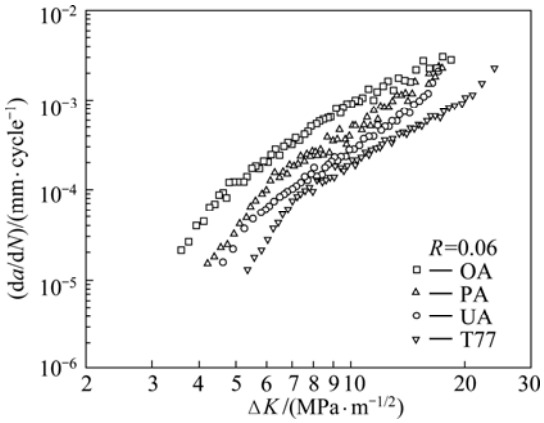

Fig.2 Fatigue crack growth rate for alloys in different ageing conditions

Table 2 Values of da/dN corresponding to various ΔK levels in Paris region

Condition	da/dN in Paris region/(mm·cycle^{-1})		
	ΔK = 8 MPa·m$^{-1/2}$	ΔK = 10 MPa· m$^{-1/2}$	ΔK = 14 MPa· m$^{-1/2}$
Over-ageing	5.32×10^{-4}	9.69×10^{-4}	1.73×10^{-3}
Peak-ageing	2.61×10^{-4}	4.81×10^{-4}	1.13×10^{-3}
Under-ageing	1.43×10^{-4}	2.65×10^{-4}	7.24×10^{-4}
T77	1.01×10^{-4}	1.98×10^{-4}	4.19×10^{-4}

levels between 8 and 14 MPa·m$^{-1/2}$, corresponding to Fig.2. A comparison among the four ageing conditions of the alloy at various ΔK levels reveals that the crack growth rate of over-aged sample is much higher than that of T77 treated ones for the same ΔK. The crack growth rates of peak aged and under-aged samples are between those of the over-aged and T77 ones, and the under-aged sample exhibits a slightly lower fatigue crack growth rate than the peak-aged one. It indicates that the T77 temper offers the best fatigue crack growth resistance, the under-ageing comes next and the over-ageing shows the worst.

Figs.3−6 show the microstructures of samples with under-ageing, peak-ageing, over-aging and T77 temper, respectively. As for the under-aged sample, it is observed that very small precipitates uniformly distribute in the Al matrix, as shown in Fig.3(a). The average size is approximately 3 nm in length and 1 nm in width. The corresponding selected area diffraction pattern (SADP) in $\langle001\rangle_{Al}$ projection is shown in Fig.3(b). Apart from the diffraction spots of the Al matrix and Al_3Zr, another two sets of diffraction patterns could be observed. One is located at {1, (2n+1)/4, 0}, the other is located at 1/3 and 2/3 of {220}. According to the results of other researchers[19], the former is from GPI zones, and the later is corresponding to η' precipitates. It is indicated that the main precipitates in under-aged sample are GPI zones and η' precipitates. HRTEM image of η' precipitates shows that the rod-like η' precipitates are fully coherent with Al matrix lattice, as shown in Fig.3(c). As for peak- aged sample, the precipitates are larger than those in the under-aged one, as shown in Fig.4(a). The sizes of η' precipitates are approximately 5 nm in length and 1.2 nm in width.

According to the SADP in $\langle001\rangle_{Al}$ projections (Fig.4(b)), the main precipitates inside the grains are also GPI zones and η' precipitates. The HRTEM image reveals that some η' phases (marked with arrow 2 in Fig.4(c)) are found to have lower coherency with Al matrix lattice although η' phase (marked with

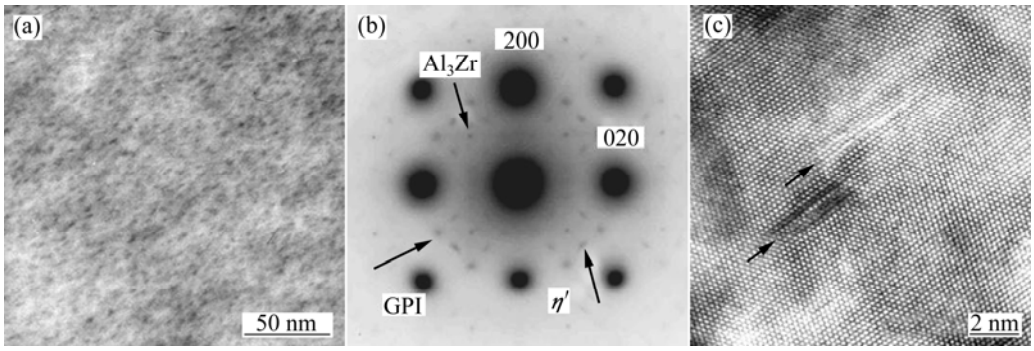

Fig.3 $[110]_{Al}$ TEM image (a), $[001]_{Al}$ SADP (b) and $[011]_{Al}$ HRTEM image of η' phases (c) of inside grains of sample after under-ageing treatment

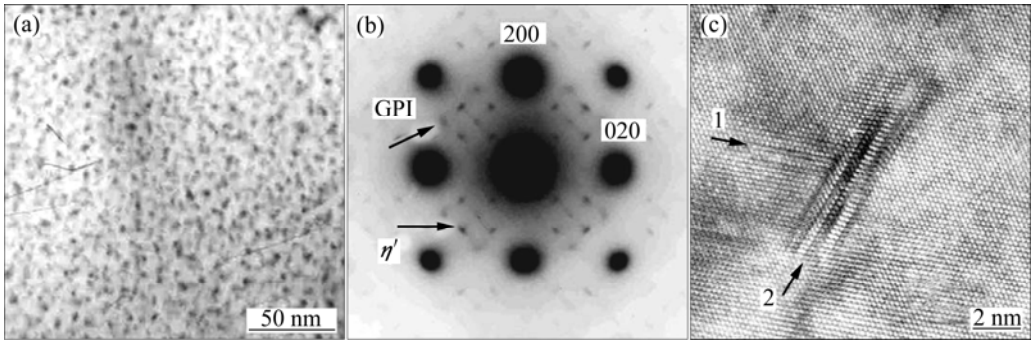

Fig.4 $[110]_{Al}$ TEM image (a), $[001]_{Al}$ SADP (b) and $[011]_{Al}$ HRTEM image of η' phases (c) of inside grains of sample after peak ageing treatment

arrow 1 in Fig.4(c)) which is fully coherent with Al matrix is also observed. As for the over-aged sample, the precipitates inside grains are much larger than those in under-aged and peak-aged ones and the average size is approximately 13 nm in length and 4 nm in width, as shown in Fig.5(a). The diffraction spots at 1/3 and 2/3 of {220} positions in the $\langle 001\rangle_{Al}$ projection (Fig.5(b)) are more complicate compared with that observed in Fig.4(b). It is indicate that η phase is the main phase in over-aged sample. According to the HRTEM image, η phase is incoherent with Al matrix lattice, as shown in Fig.5(c). As for the T77 sample, the size of the precipitates is slightly smaller than that of the over-aged sample, and more rod-like η' phases with size approximately 8 nm in length and 2 nm in width could be observed, as shown in Fig.6(a). The SADP in $\langle 001\rangle_{Al}$ projections shows that η' phase is the only precipitate in T77 samples, as shown in Fig.6(b). Furthermore, HRTEM observation shows that η' is fully coherent with Al matrix lattice in T77 condition, as shown in Fig.6(c), which is consistent with SRIVATSAN's result [12].

Fig.7 shows the grain boundary precipitates and precipitate free zones (PFZs) in under-aged, over-aged and T77 treated samples, respectively. Compared to the under-aged sample, the over-aged and T77 treated ones are characterized by a pronounced PFZ adjacent to the

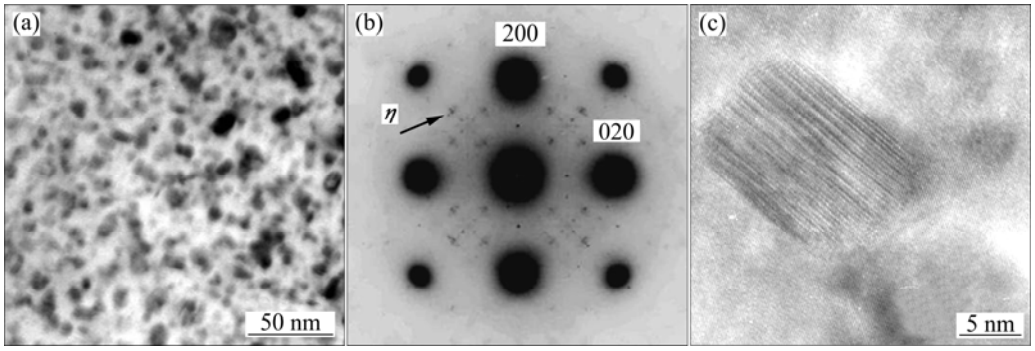

Fig.5 $[110]_{Al}$ TEM image (a), $[001]_{Al}$ SADP (b) and $[011]_{Al}$ HRTEM image of η phase (c) of inside grains of sample after over-ageing treatment

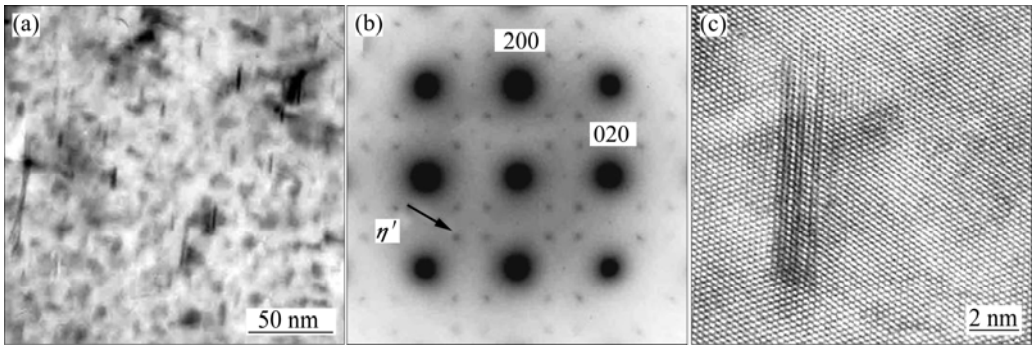

Fig.6 $[110]_{Al}$ TEM image (a), $[001]_{Al}$ SADP (b) and $[011]_{Al}$ HRTEM image of η' phase (c) of inside grains of sample after T77 treatment

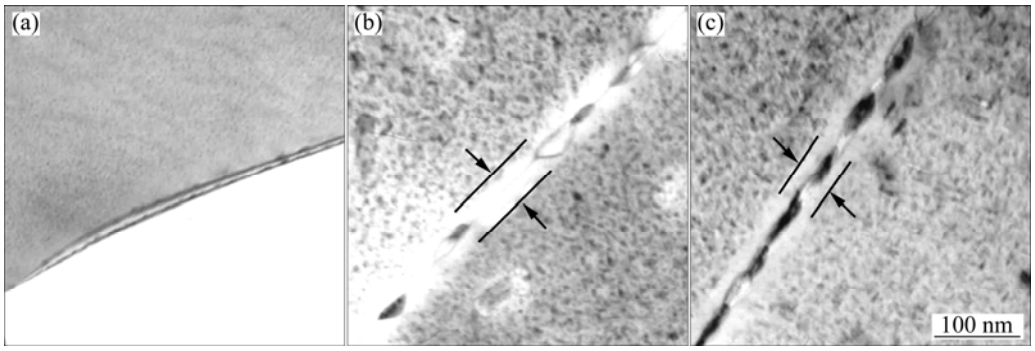

Fig.7 TEM images of precipitates in grain boundary and precipitate free zones in samples under different ageing conditions: (a) under-ageing; (b) over-ageing; (c) T77 temper

grain boundary and coarse η precipitates in grain boundary. Furthermore, the size and morphology of the grain boundary precipitates as well as the width of the PFZ in both over-aged and T77 treated samples are comparable.

4 Discussion

The present results demonstrate that 7055 Al alloys in different ageing conditions exhibit different fatigue crack growth rates. It can be explained on the basis of the microstructures that were developed during different ageing treatments. According to the works by HORNBOGEN and ZUM GAHR[20], the shearable precipitates may promote a planar dislocation distribution. When a cyclic loading is applied, a certain number of dislocations are able to move backwards during unloading on the same slip plane during the forward motion in the rising part of a loading cycle. Some of these dislocations therefore leave the material at the crack tip and thus do not contribute to crack growth. For the non-shearable precipitates, however, the dislocations have to bypass them during the rising part of the loading cycle. It is hard for the dislocations to move backwards on the original slip plane during unloading. Therefore, a large number of dislocations will be concentrated at the crack tip, which would result in a high crack growth rate. In fact, it is the reversibility of dislocation motion that controls the fatigue crack growth rate of the alloy.

According to the above statements, the degree of coherency of the precipitates with the Al matrix would be considered the first influence on the fatigue crack growth rate of the alloy. In the present work, due to the coherency of the main precipitates with the Al matrix lattice for under-ageing and T77 conditions (shown in Figs.3(c) and 6(c)), these precipitates are mainly sheared by the dislocations, promoting planar slip and enhancing the reversibility of dislocation motion. Therefore, the fatigue crack growth rates of under-aged and T77 treated samples are low. As for peak-ageing condition, in contrast, some η' precipitates that have a lower degree of coherency with Al matrix lattice form (Fig.4) and they would be non-shearable, resulting in a higher fatigue crack growth rate of peak-aged sample as compared with the under-aged and T77 treated ones, as shown in Fig.2. The over-aged sample shows the highest crack growth rate because the main precipitate is η phase, which is incoherency with Al matrix lattice (Fig.5(c)) and not shearable in nature. Therefore, the reversibility of dislocation motion during the unloading is reduced by the η phases. On the other hand, the coarser and non-shearble η particles which form within the grain of the over-aged materials may promote void formation by continued plastic flow around them, which makes the fatigue crack propagate at a much higher rate[8].

Furthermore, the size of the precipitates would also influence the fatigue crack growth rate of the alloy. According to the results of KRUEGER et al[21], the dislocation reversal was less prevalent for the small precipitates since their movement was not restricted to a single plane and probably included cross-slip. Reduced reversibility therefore would result in more rapid crack growth. It can explain the T77 treated sample shows a slightly lower crack growth rate than that of under-aged sample (Fig.2), although the main precipitates are fully coherent with Al matrix lattice in the present work. Comparing Fig.3(a) with Fig.6(a), it can be seen that the size of precipitates in under-aged sample is smaller than that in T77 treated sample, which indicates that when the precipitate is coherent with the Al matrix, the larger the precipitate is, the slower the fatigue crack grows.

On the other hand, the precipitates in grain boundary and PFZ adjacent to the grain boundary may also influence the fatigue crack growth rate[8]. It is known that the soft PFZ adjacent to the grain boundary offers less resistance to the deformation as compared to the grain interior. Therefore, it leads to easy formation of voids on coarse grain boundary particles and promotes the crack propagation. In the present work, compared to the under-aged sample, the T77 treated sample is characterized by a pronounced PFZ adjacent to the grain boundary and coarse precipitates in grain boundary (Figs.7(a) and (c)). The crack growth rate of the T77 treated sample is higher than that of the under-aged one. However, it is found that the crack growth rate of the under-aged sample is higher than that of the T77 treated one. It indicates that the effects of grain boundary precipitates and PFZ on the fatigue crack growth resistance are less significant than that of precipitates within grain in the alloy, which was discussed previously and evidenced by comparing Fig.7(b) with Fig.7(c). Although the features of the grain boundary for both over-aged and T77 treated samples are comparable, the fatigue crack growth rate of the T77 treated sample is much lower than that of the over-aged sample, which would attribute to the nature of the precipitates inside grains.

5 Conclusions

1) The ageing precipitates inside grains have an obvious effect on the fatigue crack growth resistance of 7055 Al alloy. The crack growth resistance is higher for the under-aged and T77 treated samples in which the precipitates have a high coherency with Al matrix lattice. The crack growth rate resistance of the peak-aged and over-aged samples in which the main precipitates

exhibits a lower coherency with Al matrix lattice is lower.

2) When the precipitate is coherent with Al matrix lattice, the larger the precipitate is, the slower the fatigue crack grows.

3) The effect of grain boundary precipitates and PFZ adjacent to the grain boundary on the crack growth resistance is not significant as compared with that of the precipitates inside grains.

References

[1] LIU J. Advanced aluminum and hybrid aerostructures for future aircraft [J]. Mater Sci Forum, 2006, 519/521: 1233−1238.

[2] HANLON T, KWON Y N, SURESH S. Grain size effects on the fatigue response of nanocrystalline metals [J]. Scripta Mater, 2003, 49(7): 675−680.

[3] CHEN D L, CHATURVEDI M C. Near-threshold fatigue crack growth behavior of 2195 aluminum-lithium-alloy—prediction of crack propagation direction and influence of stress ratio [J]. Metall Mater Trans A, 2000, 31(6): 1531−1541.

[4] Mc MASTER F J, TABRETT C P, SMITH D J. Fatigue crack growth rates in Al-Li alloy, 2090: Influence of orientation, sheet thickness and specimen geometry [J]. Fatigue Fract Eng Mater Struct, 1998, 21(2): 139−150.

[5] CHEN D L, CHATURVEDI M C, GOEL N, RICHARDS N L. Fatigue crack growth behavior of X2095 Al-Li alloy [J]. Int J Fatigue, 1999, 21(10): 1079−1086.

[6] ZHANG Gou-jun, LIU Gang, DING Xiang--dong, SUN Jun, TONG Zhen-feng, SHAO Yue-feng, CHEN Kang-hua. A fatigue model of high strength Al alloys containing second phase particles of various sizes [J]. Rare Metal Materings Eng, 2004, 33(1): 35−39. (in Chinese)

[7] LINDIGKEIT J, GYSLER A, LUTJERING G. Effect of microstructure on the fatigue crack propagation behavior of an Al-Zn-Mg-Cu alloy [J]. Metall Trans A, 1981, 12(9): 1613−1619.

[8] DESMUKHA M N, PANDEY R K, MUKHOPADHYAY A K. Effect of aging treatments on the kinetics of fatigue crack growth in 7010 aluminum alloy [J]. Mater Sci Eng A, 2006, 435/436(5): 318−326.

[9] LI Hai, WANG Zhi-xiu, ZHENG Zi-qiao. Influence of pre-deformation and aging on properties and microstructures of 7055 Al alloy [J]. Rare Metal Mater Eng, 2006, 35(8): 1276−1279. (in Chinese)

[10] ZHENG Zi-qiao, LI Hong-ying, MO Zhi-min. Retrogression and reaging treatment of a 7055 type aluminum alloy [J]. The Chinese Journal of Nonferrous Metals, 2001, 11(5): 771−776. (in Chinese)

[11] CHEN Jun-zhou, ZHEN Liang, SHAO Wen-zhu, DAI Sheng-long, CUI Yue-xian. Through-thickness texture gradient in AA 7055 aluminum alloy [J]. Mater Lett, 2008, 62(1): 88−90.

[12] SRIVATSAN T S, SRIRAM S. Microstructure, tensile deformation and fracture behavior of aluminum alloy 7055 [J]. J Mater Sci, 1997, 32(11): 2883−2894.

[13] Al-RUBAIE K S, BARROSO E K L, GODEFROID L B. Statistical modeling of fatigue crack growth rate in pre-strained 7475-T7351 aluminum alloy [J]. Mater Sci Eng A, 2008, 486(1/2): 585−595.

[14] SCHUBBE J J. Fatigue crack propagation in 7050-T7451 plate alloy [J]. Eng Fract Mech, 2009, 76(8): 1037−1048.

[15] PARIS P C, TADA H, DONALD J K. Service load fatigue damage—A historical perspective [J]. Int J Fatigue, 1999, 21(S1): 35−46.

[16] NOROOZI A H, GLINKA G, LAMBERT S. A two parameter driving force for fatigue crack growth analysis [J]. Int J Fatigue, 2005, 27(10/11/12): 1277−1296.

[17] DIXIT M, MISHRA R S, SANKARAN K K. Structure-property correlations in Al 7050 and Al 7055 high-strength aluminum alloys [J]. Mater Sci Eng A, 2008, 478(1/2): 163−172.

[18] HUANG Min, CHEN Jun-zhou, DAI Sheng-long, ZHEN Ling, YANG Show-jie. Effect of aging condition on fatigue crack growth in 7055 aluminum alloy [J]. J Aero Mater, 2008, 28(6): 23−26. (in Chinese)

[19] SHA G, CEREZO A. Early-stage precipitation in an Al-Zn-Mg-Cu alloy (7050) [J]. Acta Mater, 2004, 52(15): 4503−4516.

[20] HORNBOGEN E, ZUM GAHR K H. Microstructure and fatigue crack growth in a γ-Fe-Ni-Al alloy [J]. Acta Metall, 1976, 24(6): 581−592.

[21] KRUEGER D D, ANTOLOVICH STEPHEN D, VAN STONE R H. Effects of grain size and precipitate size on the fatigue crack growth behavior of alloy 718 at 427 ^{o}C [J]. Metall Trans A, 1987, 18(8): 1431−1449.

(Edited by FANG Jing-hua)